VSP

Advanced Powder Technology 19 (2008) 321–334

Advanced Powder Technology
www.brill.nl/apt

Original paper

Particle Size Distribution in Gas-phase Polyethylene Reactors

Omid Ashrafi, Hassan Nazari-Pouya, Navid Mostoufi * and Rahmat Sotudeh-Gharebagh

Process Design and Simulation Research Center, Department of Chemical Engineering, University of Tehran, PO Box 11365/4563, Tehran, Iran

Received 28 December 2006; accepted 6 August 2007

Abstract

A population balance model is developed to investigate the particle size distribution (PSD) developments in a gas-phase fluidized bed ethylene polymerization reactor. The model considers the combined effects of particle growth and elutriation for size-distributed prepolymer feed. In the proposed model, the bed is divided into several perfectly mixed serial sections. The population balance differential equations written for each section were simultaneously solved to determine the density function of the size distrubution of the polymer particles in each section. The model is able to predict the profiles of the PSD along the reactor height. It was shown that the mean size of the particles is larger at the bottom of the bed and becomes smaller when moving toward the top of the reactor. The size distribution of the polymer particles in the product becomes sharper and their mean size decreases by increasing the superficial gas velocity. Also, the mean size of the particles in the product increases by increasing the temperature of the reactor.

Keywords

Polymerization, polyethylene, fluidized bed, particle size distribution

Nomenclature

A_i coefficient used in equations (kg m^3/s)

A_{bed} bed cross-section area (m^2)

D diameter of particle (m)

D_{min} minimum particle diameter (m)

D_{max} maximum particle diameter (m)

* To whom correspondence should be addressed. E-mail: mostoufi@ut.ac.ir

 DOI:10.1163/156855208X314967

D_{bed} bed diameter (m)

D_{cat} diameter of catalyst (m)

F_c inlet mass flow of prepolymer to bed (kg/s)

F_e elutriated mass flow of polymer from the reactor (kg/s)

F_i mass flow of polymer leaving CSTR i (kg/s)

F_{in} inlet mass flow of prepolymer to bed (kg/s)

F_{out} product mass flow of polymer from bed (kg/s)

H height of the bed (m)

kp_{Ti} propagation constant [m^3/(kmol s)]

Kr^* rate of elutriation (1/s)

Ki^* elutriation rate constant [kg/(m^2 s)]

k agglomeration constant [kg/(m s)]

M_i concentration of monomer type i (kmol/m^3)

$(Mw)_k$ molecular weight of monomer k (kg/kmol)

$p_e(D)$ density function in elutriation stream (1/m)

$p_o(D)$ density function in feed (1/m)

$p_i(D)$ density function of outlet stream from reactor i (1/m)

R_n rate of consumption of component i (kmol/s)

R^i_{poly} rate of polymerization in CSTR i [kg/(kg cat s)]

t time (s)

T temperature (°C)

U_0 superficial gas velocity (m/s)

U_t terminal velocity of particles (m/s)

W weight of particles in each CSTR (kg)

X_{in} mass fraction of catalyst in inlet stream (–)

$Y(0, j)$ zeros moment of living polymer chain (kmol)

Greek

ρ_g gas density (kg/m^3)

ρ_p polymer density (kg/m^3)

ρ_{cat} catalyst density (kg/m^3)

ψ_p rate of particle growth (m/s)

ψ_{at} rate of particle corrosion due to attrition (m/s)

ψ_{ag} rate of particle growth due to agglomeration [1/(m s]

Subscripts

poly polymer

cat catalyst

j active site type number

m number of types of monomers

NS number of types of active sites

n monomer number

1. Introduction

Gas-phase ethylene polymerization has been long recognized as one of the main processes for producing polyethylenes. In this process, small catalyst particles (20–80 μm in diameter) as prepolymers are continuously fed into a fluidized bed and react with the incoming fluidizing gas (monomers) to form polymer particles in the size range of 100–5000 μm. The performance of the fluidized bed reactor strongly depends on the hydrodynamic parameters such as minimum fluidization velocity, size of bubbles, and gas–solid mass and heat transfer coefficients. These hydrodynamic parameters, in turn, depend on the particle size distribution (PSD). In other words, the PSD and the flow rate of gas determine the hydrodynamic state of the bed. Therefore, a mathematical model capable of predicting the PSD is essential to understand and to optimize the performance of these reactors. However, most of the existing models for predicting the properties of the product and performance of the reactor assume a constant polymer particle diameter and do not account for PSD in the bed [1–4].

Obtaining the PSD using the population balance mobel (PBM) has been studied by a number of researchers. Zacca *et al.* [5] developed the PBM using catalyst residence time to model particle size developments in multistage olefin polymerization reactors. Choi *et al.* [6] followed the population balance approach of Kunii and Levenspiel [7] to investigate the effect of feed catalyst size distribution on the PSD of the polyolefin produced in a fluidized bed reactor for both non-deactivated and deactivated catalysts. Khang and Lee [8] applied a population balance approach to investigate the effect of non-ideal mixing behavior of solid particles on the PSD in the fluidized bed of olefin polymerization reactor. Hatzantonis *et al.* [9] formulated and solved the generalized steady-state PBM by counting the effect of particle

growth, catalyst deactivation, particle attrition, agglomeration and particle elutriation on the PSD in gas-phase olefin polymerization. Harshe *et al.* [10] presented a comprehensive computational model for predicting the PSD and performance of the fluidized bed of a polypropylene reactor. They solved mass and energy balances, the PBM and the hydrodynamics model simultaneously.

There have been also a number of papers investigating the PSD under different conditions. Yiannoulakis *et al.* [11] developed a PBM to predict the PSD in an ethylene copolymerization fludized bed reactor under particle agglomeration conditions. They showed that under the well-mixed condition, internal and external heat and mass transfer limitations have an impotant effect on the PSD of the product. Kotoulas *et al.* [12] developed a comprehensive PBM to predict the dynamic evolution of the PSD in high hold-up non-reactive liquid–liquid dispersions and reactive liquid (solid)–liquid suspension polymerization systems. They used the fixed pivot numerical method for solving the population balance equation. Alexopoulos *et al.* [13, 14] provided a comprehensive investigation on the numerical problems arising in the solution of dynamic population balance equations (PBEs) for particulate processes undergoing simultaneous particle growth and aggregation. A detailed investigation on the effect of different particle growth rate functions on the calculated PSD was carried out over a wide range of variation of dimensionless aggregation and growth times. Roussos *et al.* [15] presented a comprehensive investigation on the numerical solution of the dynamic PBE in batch and continuous flow particulate processes, and solved it using the Galerkin method for particulate processes undergoing simultaneous particle aggregation, growth and nucleation. For continuous particulate processes, they investigated the effect of various size-dependent particle growth models on the calculated steady-state PSDs.

In the present study, a PBM is developed in accordance with the hydrodynamic model of Alizadeh *et al.* [4]. In this hydrodynamic model, it was assumed that the fluidized bed reactor for ethylene production would be divided into serial continuously stirred tank reactors (CSTRs). The PBM differential equations were then developed for each cell and simultaneously solved together to determine the PSD profiles of the polyethylene product. The model is able to predict the axial profile of the mean particle diameter.

2. Modell Development

2.1. Hydrodynamics

Alizadeh *et al.* [4] showed that a fluidized bed reactor of ethylene polymerization could be considered as a series of CSTRs. They considered the polyethylene reactor to consist of three CSTRs in series. Nevertheless, Kiashemshaki *et al.* [16] later showed that the fluidized bed reactor used for gas-phase polyethylene production should be divided into four segments. Therefore, in the present study, the polyethylene reactor is considered to consist of four CSTRs in series, as shown in

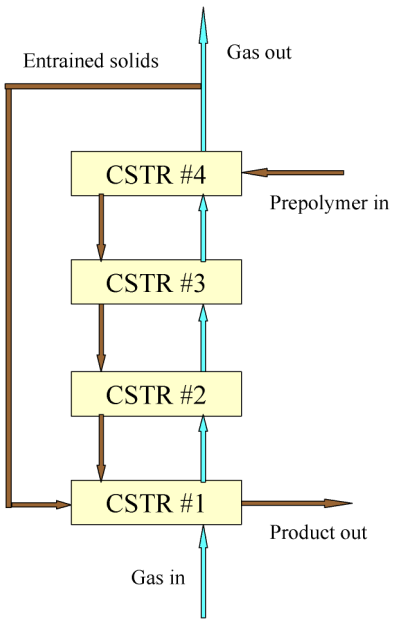

Figure 1. Schematic diagram of the modeling structure. This figure is published in color on http://www.ingentaconnect.com/content/vsp/apt

Fig. 1. The feed to the reactor enters at the top (CSTR #4) and the product leaves the reactor from the bottom (CSTR #1).

2.2. Kinetics

In the present study, the comprehensive mechanism of McAuley *et al.* [17] was used to describe the copolymerization kinetics of ethylene with 1-butene over a Ziegler–Natta catalyst with two different catalyst sites. This mechanism comprises of a series of elementary reactions such as initiation, propagation and chain transfer. Application of the method of moments enables prediction of the overall reaction rate for each component [17]:

$$R_n = \sum_{j=1}^{NS} \sum_{n=1}^{m} [M_n] Y(0, j) k p_{Tn}(j), \quad n = 1, 2. \tag{1}$$

The cumulative rate of polymer production is calculated from the following:

$$R_{\text{poly}} = \sum_{n=1}^{m} (\text{Mw})_n R_n. \tag{2}$$

In the population balance, the rate of growth of the particles due to polymerization could be obtained from the production rate of the polymer evaluated in (2).

2.3. PBM

As stated in the hydrodynamics section, the reactor consists of CSTRs in series. A single CSTR is shown in Fig. 2 in its general form with all possible solid streams. Catalyst particles (as prepolymer) are fed into the bed with a constant flow rate F_{in}. The mass of the bed, W, is kept constant by controlling the product withdrawal rate F_{out}. Inside the bed, the particles may simultaneously grow in size due to polymerization and agglomeration, and break into smaller particles due to attrition. The rate of entrainment by fluidizing gas from this segment is F_{e}. For the sake of simplicity, particles are assumed to be spherical with constant density. The PSD in the reactor is specified by the statistical density function, $p_i(D)$. Note that due to the well-mixed assumption for the particles in each CSTR, the density function of the particles in the outlet stream is identical to that in the bed, $p_i(D)$.

The steady-state mass balance for particles in the size range $[D, D + \Delta D]$ is:

$$\begin{aligned}
&\left(\begin{array}{c}\text{Particles entering}\\ \text{with catalyst feed}\end{array}\right) - \left(\begin{array}{c}\text{Particles leaving}\\ \text{in the product stream}\end{array}\right) - \left(\begin{array}{c}\text{Particles leaving}\\ \text{in the elutriation stream}\end{array}\right)\\
&\quad + \left(\begin{array}{c}\text{Particles entering the}\\ \text{interval from a smaller size}\\ \text{due to polymerization}\end{array}\right) - \left(\begin{array}{c}\text{Particles leaving the}\\ \text{interval to a larger size}\\ \text{due to polymerization}\end{array}\right)\\
&\quad + \left(\begin{array}{c}\text{Particles entering the}\\ \text{interval from a larger size}\\ \text{due to attrition}\end{array}\right) - \left(\begin{array}{c}\text{Particles leaving the}\\ \text{interval to a smaller size}\\ \text{due to attrition}\end{array}\right)\\
&\quad + \left(\begin{array}{c}\text{Generation of particle mass}\\ \text{within the interval}\\ \text{due to polymerization}\end{array}\right) - \left(\begin{array}{c}\text{Loss of particle mass}\\ \text{within the interval}\\ \text{due to attrition}\end{array}\right)\\
&\quad + \left(\begin{array}{c}\text{The net rate of change of the number volume density}\\ \text{function due to agglomeration}\end{array}\right) = 0.
\end{aligned} \tag{3}$$

By arranging the above formula in mathematical form, the following differential

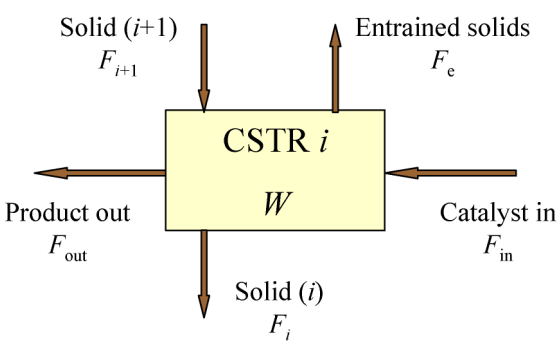

Figure 2. Schematic diagram of one CSTR with all possible solid streams. This figure is published in color on http://www.ingentaconnect.com/content/vsp/apt

equation of population balance could be obtained:

$$\left(\frac{F_c}{W}\right)p_o(D) - \left(\frac{F_i}{W} + Kr^*(D)\right)p_i(D) - \frac{d}{dr}[p_i(D)\psi_p(D)] + \frac{d}{dr}[p_i(D)\psi_{at}(D)] + p_i(D)\frac{3}{D}[\psi_p(D) - \psi_{at}(D)] + \psi_{ag} = 0. \quad (4)$$

In order to obtain the equations of the model in this study, the terms in (4) were determined for each segment as follows:

- Assuming that the diameter of the particle at every moment is D, the rate of growth of particles due to polymerization could be written as [9]:

$$\psi_p = \frac{D_{cat}^3}{3D^2}\frac{\rho_{cat}}{\rho_p}R_{poly}. \quad (5)$$

- The growth of particles due to agglomeration in the reactor could be obtained from [9]:

$$\psi_{ag} = k\frac{3D^3}{\pi\rho_p}\int_{D_{min}}^{\sqrt[3]{D^3 - D_{min}^3}}(d^4 + D'^4)\left(\frac{1}{d^3} + \frac{1}{D'^3}\right)\frac{p_i(D)}{d^5}\frac{p_i(D')}{D'}\,dD' + k\frac{6p_i(D)}{\pi\rho_p}\int_{D_{min}}^{D_{max}}(D^4 + D'^4)\left(\frac{1}{D^3} + \frac{1}{D'^3}\right)\frac{p_i(D')}{D'^3}\,dD', \quad (6)$$

where $d = \sqrt[3]{D^3 - D'^3}$, D_{min} is the minimum particle diameter and D_{max} is the maximum particle diameter. The agglomeration constant, k, for polyethylene has been reported by Arastoopour *et al.* [19].

- The attrition depends mainly to the physical properties of the particle material rather than its size. Therefore, the attrition term in (4) was assumed to be constant [9].

- The flux of particles carried out of the bed due to entrainment could be obtained from the following:

$$F_e p_e(D) = WKr^*(D)p_4(D), \quad (7)$$

where the elutriation rate constant is evaluated from [7]:

$$Kr^* = Ki^*\frac{A_{bed}}{W}, \quad (8)$$

and:

$$Ki^* = 23.7\rho_g U_0 \exp\left(-\frac{5.4U_t}{U_0}\right). \quad (9)$$

Elutriated solids are recycled to the bottom of the fluidized bed and recycled to the bottom of the bed (CSTR #1).

Selçuk *et al.* [19] developed a computationally efficient approach for the solution of population balance of Kunii and Levenspiel [7]. This new approach replaces the conventional numerical integration of the analytical solution of the population balance with direct integration in ordinary differential equation form by using a powerful integration. Following the approach of Selçuk *et al.* [18], the steady state population balance (4) could be written for each CSTR of Fig. 1. Using the relationships described above, equations for all sections would be simplified to the followings:

CSTR #1:

$$\frac{\mathrm{d}p_1(D)}{\mathrm{d}D} = \frac{1}{A_1/D^2 - \psi_{\mathrm{at}}}\left\{\frac{F_2}{W}p_2(D) + \left(\frac{5A_1}{D^3} - \frac{F_1}{W} - \frac{3\psi_{\mathrm{at}}}{D}\right)p_1(D) + Kr^* p_4(D) + \psi_{\mathrm{ag}}\right\}, \tag{10}$$

CSTR #2:

$$\frac{\mathrm{d}p_2(D)}{\mathrm{d}D} = \frac{1}{A_2/D^2 - \psi_{\mathrm{at}}} \times \left\{\frac{F_3}{W}p_3(D) + \left(\frac{5A_2}{D^3} - \frac{F_2}{W} - \frac{3\psi_{\mathrm{at}}}{D}\right)p_2(D) + \psi_{\mathrm{ag}}\right\}, \tag{11}$$

CSTR #3:

$$\frac{\mathrm{d}p_3(D)}{\mathrm{d}D} = \frac{1}{A_3/D^2 - \psi_{\mathrm{at}}} \times \left\{\frac{F_4}{W}p_4(D) + \left(\frac{5A_3}{D^3} - \frac{F_3}{W} - \frac{3\psi_{\mathrm{at}}}{D}\right)p_3(D) + \psi_{\mathrm{ag}}\right\}, \tag{12}$$

CSTR #4:

$$\frac{\mathrm{d}p_4(D)}{\mathrm{d}D} = \frac{1}{A_4/D^2 - \psi_{\mathrm{at}}} \times \left\{\frac{F_c}{W}p_0(D) + \left(\frac{5A_4}{D^3} - \frac{F_4}{W} - Kr^* - \frac{3\psi_{\mathrm{at}}}{D}\right)p_4(D) + \psi_{\mathrm{ag}}\right\}, \tag{13}$$

where:

$$A_i = \frac{D_{\mathrm{cat}}^3}{3}\frac{\rho_{\mathrm{cat}}}{\rho_{\mathrm{p}}}R_{\mathrm{ploy}}. \tag{14}$$

By solving the ordinary differential equations (10)–(14) simultaneously, the density functions for outlet streams of all segments would be obtained. The PSD of the final product stream out of the bed is given by $p_1(D)$.

3. Results and Discussion

The model equations were solved for the operating conditions shown in Table 1. A sample of linear low-density polyethylene (LLDPE) produced at such operating conditions was also obtained from an industrial plant. A comparison between the actual PSD of the polymer and the PSD calculated by the model is shown in Fig. 3 in terms of cumulative PSD. The actual cumulative PSD of the feed is also shown in Fig. 3. It can be seen in Fig. 3 that the calculated PSD is in fair agreement with the actual PSD. However, the calculated PSD is somehow sharper than the actual

Table 1.
Parameters used in the simulation

Parameter	Value	Unit
ρ_g	21	kg/m^3
ρ_{cat}	2840	kg/m^3
ρ_p	920	kg/m^3
D_{bed}	4.8	m
H	14	m
U_0	0.5	m/s
T	72	°C
ψ_{at}	10^{-6}	kg/s
k	10^{-7}	kg/(m s)
F_{in}	0.5	kg/s

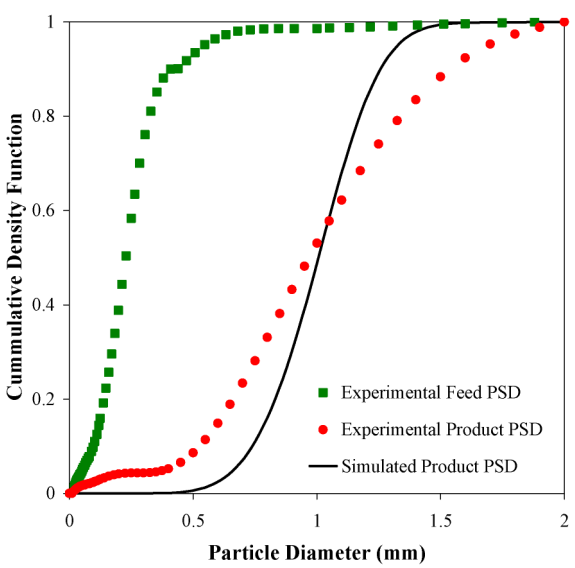

Figure 3. Comparison between actual and simulated PSDs. This figure is published in color on http://www.ingentaconnect.com/content/vsp/apt

one, while the mean size is predicted correctly. In fact, Fig. 3 reveals that even though the model correctly-predicts the average growth of the polymer particles, it under-predicts the growth of the finer particles, while it over-predicts the growth of coarser particles. These deviations could be attributed to the fact that a pseudo-homogeneous hydrodynamic model has been adopted in the present work in which all particles are subject to the same growth conditions and independent of the size of the particles. In fact, smaller particles grow faster and applying a kinetic model that could distinguish between the rate of growth of particles with different sizes should be able to reduce such a deviation.

Estimated PSDs of the polymer in different CSTRs along the reactor are shown in Fig. 4 at $U_0 = 0.25$ m/s. It can be seen in Fig. 4 that at lower gas velocity, the mean size of the particles decreases when moving down the reactor. Noting that CSTR #4 is placed at the top and CSTR #1 at the bottom, and that the direction of the overall movement of the polymer particles is downward, the size of particles grows larger due to polymerization when moving down the reactor. Figure 4 also reveals that the PSD of the polymer becomes sharper when moving toward the bottom of the reactor. The reason for such a trend is that inspite of the fact that particles grow larger when moving down the reactor, the rate of production is higher for fine particles. Therefore, the finer particles (corresponding to the left tail of the PSD curve) grow faster than the larger particles (corresponding to the right tail of the PSD curve), and the PSD curve becomes less wide as the particles move down the reactor and their mean size becomes larger.

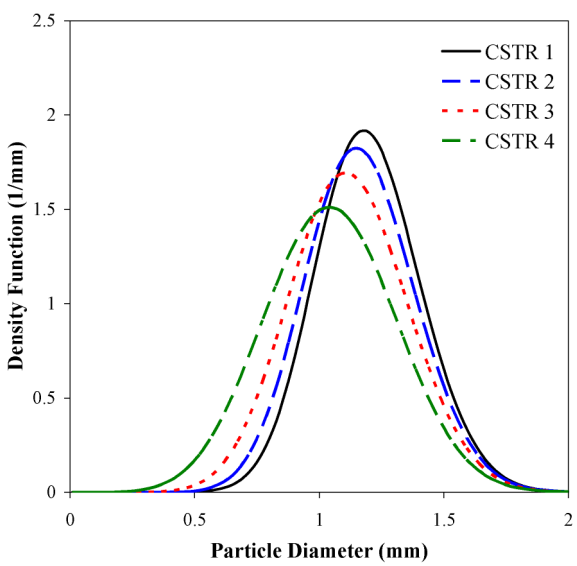

Figure 4. Predicted PSD of polymer along the height of the bed at $U_0 = 0.25$ m/s. This figure is published in color on http://www.ingentaconnect.com/content/vsp/apt

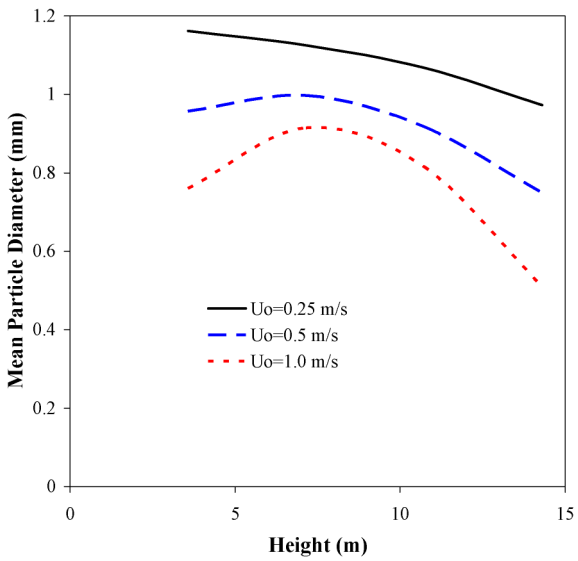

Figure 5. Axial profile of mean particle size of polymer. This figure is published in color on http://www.ingentaconnect.com/content/vsp/apt

An important outcome of the model developed in this study is that it can determine the axial profile of the PSD in the reactor. In fact, since the CSTRs in this model are located one on top of another, the mean particle size in each CSTR could be attributed to the size of the particle at the corresponding height of the bed. Figure 5 illustrates the axial profiles of the mean particle size in the reactor at different gas velocities. As can be seen in Fig. 5, finer particles are situated at the top of the reactor, while larger particles are found at the bottom. However, Fig. 5 reveals that at moderate to high superficial gas velocities, the mean size of particles at the bottom of the bed tends toward smaller values. This is due to recirculation of the entrained fine particles from the top to the bottom of the bed. By increasing the superficial gas velocity, larger amounts of fine particles are recycled from the top to the bottom of the bed, which leads to a decrease in the mean size of the particles at moderate to high gas velocity. Figure 5 also illustrates that increasing the superficial gas velocity results in decreasing the particle size in the reactor. This effect could be explained by the fact that increasing the gas velocity increases the heat removal from the reactor; thus, the temperature of the reactor, as well as the rate of reaction, decreases consequently. As a result, the mean particle size in the reactor shifts to smaller sizes by increasing the gas velocity.

The effect of superficial gas velocity in the reactor on the PSD of the product is shown in Fig. 6. As can be seen in Fig. 6, increasing the superficial gas velocity results in the PSD moving toward smaller values. This effect is already discussed in the previous figure and is a result of decreasing the temperature of the reactor based on increasing the rate of heat removal by gas convection when increasing the gas velocity. Moreover, increasing the gas velocity results in higher recycling of elutri-

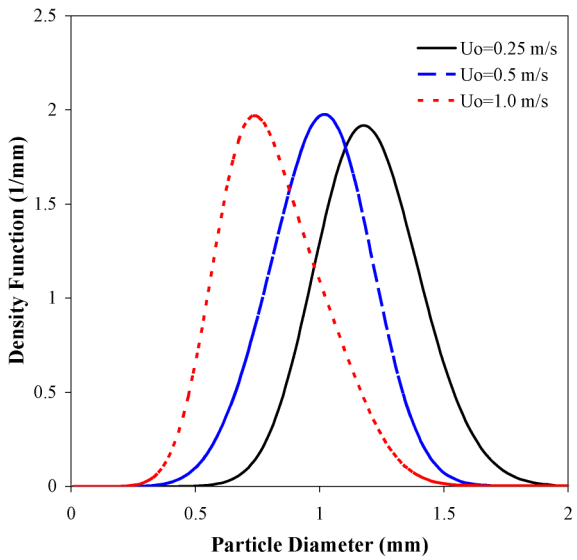

Figure 6. Effect of superficial gas velocity on the PSD of the product. This figure is published in color on http://www.ingentaconnect.com/content/vsp/apt

ated fines to the bottom of the bed, thus decreasing the mean particle size. Figure 6 also illustrates that the PSD becomes sharper when increasing the gas velocity in the reactor. This phenomenon could be explained in view of decreasing the particle size in the bed when increasing the superficial gas velocity. In fact, smaller particles grow faster. Thus, when the PDS shifts toward smaller sizes (corresponding to higher gas velocity), growth of smaller particles becomes faster than if the curve would have been located at larger sizes. Consequently, the left tail of the PSD curve would be closer to the right than at higher gas velocities and the PSD would become sharper at such a condition.

The effect of reactor temperature on the PSD of the product is illustrated in Fig. 7. It is worth noting that the rates of polymerization and agglomeration depend on temperature, but attrition was considered to be always constant. The relationship between temperature and polymerization reaction rate constants has been already reported by Kiashemshaki *et al.* [16], which has been used in this work. However, the relationship between temperature and agglomeration constant, k, has not been completely investigated yet. The effect of temperature on the agglomeration constant has been briefly investigated by Arastoopour *et al.* [19]. Assuming an Arrhenius-type temperature dependency for this consatant and using the experimental data of Arastoopour *et al.* [19], it was found that the corresponding energy of activation for agglomeration is equal to 2.21 MJ/kmol K. The same activation energy was assumed in this work when studying the effect of temperature on the agglomeration rate. According to Fig. 7, increasing the reactor temperature makes the PSD of the product wider and its mean move toward higher values. In fact,

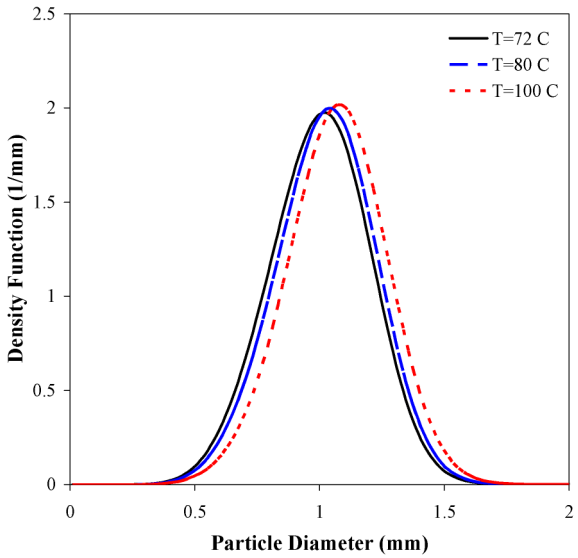

Figure 7. Effect of reactor temperature on the PSD of the product. This figure is published in color on http://www.ingentaconnect.com/content/vsp/apt

increasing the temperature of the reactor causes an increase in the rate of the polymerization reaction which results in the production of larger particles.

4. Conclusions

A mathematical model is proposed for predicting the PSD of polymer particles in the polyethylene reactor that is able to provide the profile of the particle size along the reactor hight. In this model, a generalized framework based on the CSTRs in series in the hydrodynamics model of Alizadeh *et al.* [4] and the two-site kinetic scheme of McAuley *et al.* [17] were used. It was shown that smaller particles exist at the top of the reactor, while larger particles tend to be present at the bottom. The effect of superficial gas velocity and temperature on the PSD of the product was also investigated. It was demonstrated that by increasing the superficial gas velocity, the PSD of the product becomes sharper and shifts toward smaller particles. Also, by increasing the temperature of the reactor, the PSD of the product shifts toward larger particles because the reaction rate increases; thus, larger particles are produced.

References

1. K. Y. Choi and W. H. Ray, The dynamic behaviour of fluidized bed reactors for solid catalyzed gas phase olefin polymerization, *Chem. Eng. Sci.* **40**, 2261–2279 (1985).
2. K. B. McAuley, J. P. Talbot and T. J. Harris, A comparison of two-phase and well-mixed models for fluidized-bed polyethylene reactors, *Chem. Eng. Sci.* **49**, 2035–2045 (1994).
3. F. A. N. Fernandes and L. M. F. Lona, Heterogeneous modeling for fluidized-bed polymerization reactor, *Chem. Eng. Sci.* **56**, 963–969 (2001).

4. M. Alizadeh, N. Mostoufi, S. Pourmahdian and R. Sotudeh-Garebagh, Modeling of fluidized bed reactor of ethylene polymerization, *Chem. Eng. J.* **97**, 27–35 (2004).
5. J. J. Zacca and J. A. Debling, Reactor residence time distribution effects on the multistage polymerization of olefin, *Chem. Eng. Sci.* **51**, 4859–4886 (1996).
6. K. Y. Choi, X. Zhao and S. Tang, Population balance modeling for a continuous gas phase olefin polymerization reactor, *J. App. Polym. Sci.* **53**, 1589–1597 (1994).
7. D. Kunii and O. Levenspiel, *Fluidization Engineering*, 2nd edn. Butterworth-Heinemann, Boston, MA (1991).
8. D. Y. Khang and H. H. Lee, Particle size distribution in fluidized bed for catalytic polymerization, *Chem. Eng. Sci.* **52**, 421–431 (1997).
9. H. Hatzantonis, C. Kiparissides and A. Goulas, A comprehensive model for prediction of particle size distribution in catalyzed olefin polymerization fluidized-bed reactor, *Chem. Eng. Sci.* **53**, 3251–3267 (1998).
10. Y. M. Harshe, R. P. Utikar and V. V. Ranade, A computational model for predicting particle size distribution and performance of fluidized bed polypropylene reactor, *Chem. Eng. Sci.* **59**, 5145–5156 (2004).
11. H. Yiannoulakis, A. Yiagopoulos and C. Kiparissides, Recent developments in the particle size distribution modeling of fluidized bed olefin polymerization reactors, *Chem. Eng. Sci.* **56**, 917–925 (2001).
12. C. Kotoulas and C. Kiparissides, A generalized population balance model for the prediction of particle size distribution in suspension polymerization reactors, *Chem. Eng. Sci.* **61**, 332–346 (2006).
13. A. H. Alexopoulos, A. I. Roussos and C. Kiparissides, Part I: dynamic evolution of the particle size distribution in particulate processes undergoing combined particle growth and aggregation, *Chem. Eng. Sci.* **59**, 5751–5769 (2004).
14. A. H. Alexopoulos and C. Kiparissides, Part II: dynamic evolution of the particle size distribution in particulate processes undergoing simultaneous particle nucleation, growth and aggregation, *Chem. Eng. Sci.* **60**, 4157–4169 (2005).
15. A. I. Rousses, A. H. Alexopoulos and C. Kiparissides, Part III: Dynamic evolution of the particle size distribution in particulate processes: a Galerkin on finite elements approach, *Chem. Eng. Sci.* **60**, 6998–7010 (2005).
16. A. Kiashemshaki, N. Mostoufi and R. Sotudeh-Gharebagh, Two phases modeling of a gas phase polyethylene fluidized bed reactor, *Chem. Eng. Sci.* **61**, 3997–4006 (2006).
17. K. B. McAuley, J. F. MacGregor and A. E. Hamielec, A kinetic model for industrial gas-phase ethylene copolymerization, *AIChE J.* **36**, 837–850 (1990).
18. N. Selçuk, O. Oymak and E. Değirmenci, Basic requirement for modeling fluidized beds: fast computation of particle size distribution, *Powder Technol.* **87**, 269–271 (1996).
19. H. Arastoopour, C. S. Haung and S. A. Weil, Fluidization behavior of particle under agglomerating conditions, *Chem. Eng. Sci.* **43**, 3063–3075 (1988).